N,N′-Diferrocenyl-*N*-heterocyclic Carbenes and Their Derivatives

Benno Bildstein,*,† Michael Malaun,† Holger Kopacka,† Klaus Wurst,† Martin Mitterböck,† Karl-Hans Ongania,‡ Giuliana Opromolla,§ and Piero Zanello§

Institut für Allgemeine, Anorganische und Theoretische Chemie, Universität Innsbruck, Innrain 52a, A-6020 Innsbruck, Austria, Institut für Organische Chemie, Universität Innsbruck, Innrain 52a, A-6020 Innsbruck, Austria, and Dipartimento di Chimica dell'Università di Siena, Via Aldo Moro, I-53100 Siena, Italy

Received May 20, 1999

In continuation of our work on Wanzlick/Arduengo carbenes containing redox-active ferrocenyl substituents we report on the synthesis of *N,N′*-diferrocenyl imidazol(in)ium salts as precursors of imidazol(in)-2-ylidenes. The necessary starting material for this chemistry is aminoferrocene, which was prepared by an improved and large-scale synthesis by the sequence solid lithioferrocene, iodoferrocene, *N*-ferrocenylphthalimide, aminoferrocene. The preparation of *N,N′*-diferrocenyl heterocycles involves condensation of aminoferrocene with glyoxal to afford *N,N′*-diferrocenyldiazabutadiene [Fc-DAB], reduction, condensation with formaldehyde, and oxidation with trityl salts to yield *N,N′*-diferrocenylimidazol(in)ium salts. In situ deprotonation and trapping with electrophiles yielded the expected metal complexes and derivatives in some cases [Ag^+ or S_8], but attempted reaction with other transition metals [e.g., Pd(II)] failed to give the corresponding complexes, due to (i) steric hindrance by the two *N*-ferrocenyl substituents, (ii) reduced acidity of the imidazol(in)ium precursors, and (iii) inaccessibility of the free carbenes. Spectroscopic [IR, Raman, UV−vis, MS, NMR (^{1}H, ^{13}C, ^{109}Ag)], structural [X-ray], and electrochemical [CV] properties are reported and compared to those of other *N*-heterocyclic carbene derivatives.

Introduction

Nucleophilic *N*-heterocyclic carbenes of the Wanzlick/Arduengo-type are compounds that are receiving much attention because of their interesting chemistry.[1,2] The subject of this paper is the synthesis and reactivity of *N*-heterocyclic carbenes with two *N*-ferrocenyl groups. In general, three properties distinguish ferrocenyl substituents from other, purely organic moieties: (i) unique steric bulk with special steric requirements due to the cylindrical shape, (ii) electronic stabilization of adjacent electron-deficient centers due to participation of the iron atom in the dispersal of the positive charge,[3,4] and (iii) chemical stability and reversibilty of the ferrocene/ferrocenium redox couple.[5] Earlier we reported on metallocenyl-substituted *N*-heterocyclic carbene derivatives with remote alkyl-spacered ferrocenyl substituents[6] and on benzimidazol-2-ylidene derivatives with one *N*-ferrocenyl substituent.[7] As might be anticipated, the stereoelectronic effects of the ferrocenyl groups increase with the proximity and with the number of ferrocenyl substituents; therefore *N*-heterocyclic carbenes with two *N*-ferrocenyl groups are interesting (and quite challenging) target compounds, as will be discussed in the following.

Results and Discussion

General Synthetic Strategy and Improved Large-Scale Synthesis of Functionalized Ferrocenes. Conceptually, one might assume that the most convenient and straightforward synthetic approach to *N,N′*-diferrocenyl azolium salts as precursors of the corresponding *N*-heterocyclic carbenes would be a direct substitution of a suitable imidazole synthon, e.g., cross coupling reactions of a metal imidazolide with bromo or iodoferrocene or alternatively reactions of *N*-halogeno or *N*-diazonium imidazole with metalated ferrocenes. We attempted earlier such reactions under a variety of conditions but without any positive outcome.[7] Similarly, the one-pot synthesis of *N,N′*-diferrocenyl imidazolium salts by ring-closure condensation of aminoferrocene with paraformaldehyde, ammonium chloride, and gly-

* E-mail: benno.bildstein@uibk.ac.at.
† Institut für Allgemeine, Anorganische und Theoretische Chemie, Universität Innsbruck.
‡ Institut für Organische Chemie, Universität Innsbruck.
§ Dipartimento di Chimica dell'Università di Siena.

(1) Arduengo, A. J., III; Krafczyk, R. *Chem. Z.* **1998**, *32*, 6.
(2) Herrmann, W. A.; Köcher, C. *Angew. Chem.* **1997**, *109*, 2257; *Angew. Chem., Int. Ed. Engl.* **1997**, *36*, 2162, and references therein.
(3) Lukasser, J.; Angleitner, H.; Schottenberger, H.; Kopacka, H.; Schweiger, M.; Bildstein, B.; Ongania, K.-H.; Wurst, K. *Organometallics* **1995**, *14*, 5566, and references therein.
(4) Bildstein, B.; Schweiger, M.; Kopacka, H.; Ongania, K.-H.; Wurst, K. *Organometallics* **1998**, *17*, 2414.
(5) Geiger, W. E. Organometallic Radical Processes. In *Journal of Organometallic Chemistry Library*; Trogler, W. C., Ed.; Elsevier: Amsterdam, 1990; Vol. 22, Chapter 5, p 142.
(6) Bildstein, B.; Malaun, M.; Kopacka, H.; Ongania, K.-H.; Wurst, K. *J. Organomet. Chem.* **1998**, *552*, 45.
(7) Bildstein, B.; Malaun, M.; Kopacka, H.; Ongania, K.-H.; Wurst, K. *J. Organomet. Chem.* **1999**, *572*, 177.

10.1021/om990377h CCC: $18.00
Publication on Web 09/16/1999

Scheme 1. Synthesis of Aminoferrocene

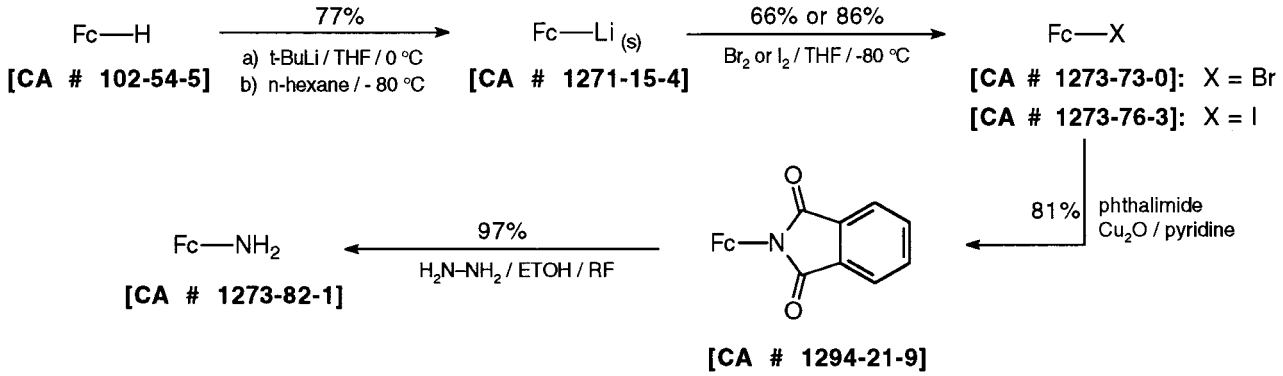

Scheme 2. Synthesis of Compounds 1−5 (Fc = ferrocenyl)

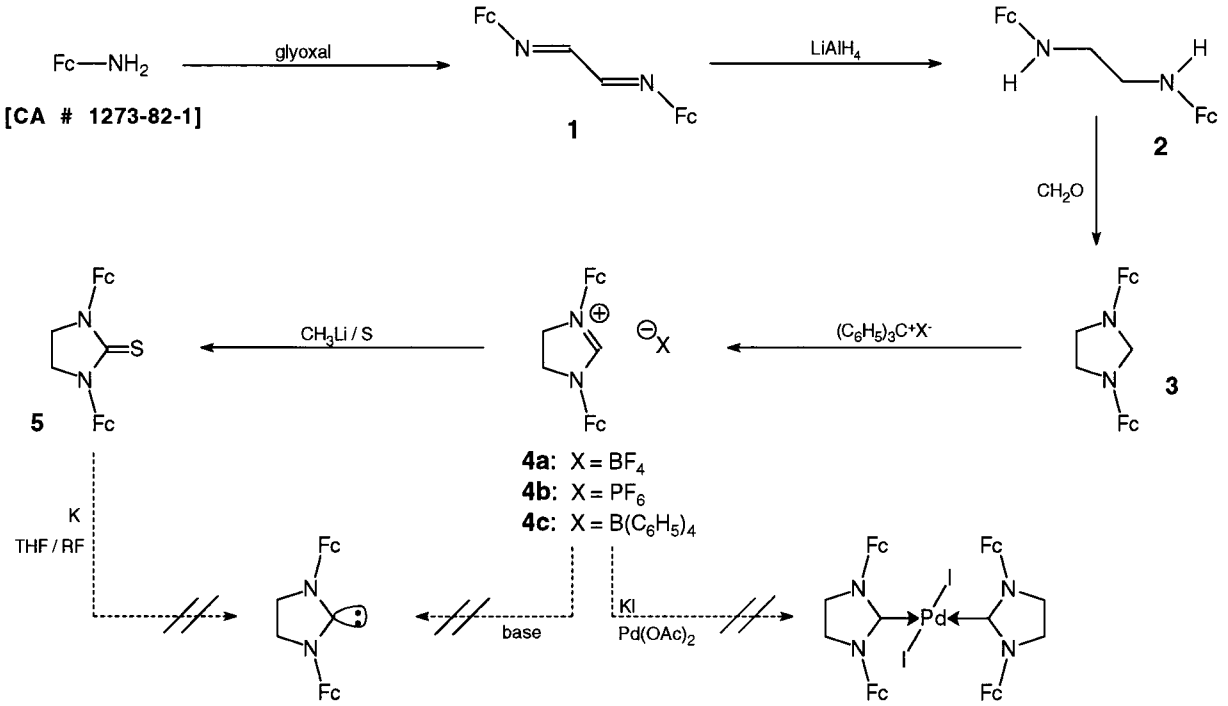

oxal failed under conditions that have been reported to yield *N*,*N*′-diarylimidazolium salts.[8] Therefore we had to develop a new approach, which is based on a stepwise formation of the heterocyclic moiety starting from aminoferrocene as the key synthon.

Although aminoferrocene is a known compound, the main drawback for further preparative work is the tedious multistage preparations of aminoferrocene starting from ferrocene with ferrocenoyl azide, *N*-ferrocenyl acetamide, or *N*-ferrocenyl phthalimide as key intermediates.[9] In our hands the best method for multigram quantities of aminoferrocene is the Gabriel synthesis[10] from *N*-ferrocenyl phthalimide,[11,12] although this route necessitates the synthesis of bromo- or iodoferrocene[11] or ferrocene boronic acid[12] as precursors of *N*-ferrocenyl phthalimide. Herein we report optimized high-yield syntheses for the large scale (> 20 g) preparation of functionalized ferrocenes and aminoferrocene by the sequence ferrocene−*solid monolithioferrocene*−iodoferrocene−ferrocenyl phthalimide−aminoferrocene (Scheme 1). The main advantages of these procedures are the selective monometalation of ferrocene and the direct bromination and iodination of lithioferrocene on a quite large scale (>30 g), avoiding some otherwise used intermediates such as ferrocene boronic acid or chloromercurioferrocene. Halogenoferrocenes and monometalated ferrocenes are probably among the most useful synthons in ferrocene chemistry; hence these results might be of general value for other workers.

Synthesis and Properties of 1,3-Diferrocenylimidazoline Compounds. The key starting material for all of the following chemistry is *N*,*N*′-diferrocenyl-1,4-diaza-1,3-butadiene (**1**) (Fc-DAB). It is easily prepared in 95% yield by condensation of aminoferrocene with aqueous glyoxal (Scheme 2). Fc-DAB (**1**) is a dark purple (λ_{max} = 524 nm) air-stable compound which not only serves as an entry into *N*-ferrocenyl-*N*-heterocyclic carbene chemistry but, in addition, is a new redox-active bidendate ligand, analogous to other DAB compounds.[13]

(8) Arduengo, A. J., III; U.S. Patent 5077414, 1991.
(9) Herberhold, M. Ferrocene Compounds Containing Heteroelements. In *Ferrocenes*; Togni, A., Hayashi, T., Eds.; VCH: Weinheim, 1995; Chapter 5, p 225.
(10) Nesmeyanow, A. N.; Ssazonowa, W. A.; Drosd, V. N. *Chem. Ber.* **1960**, *93*, 2717.
(11) Sato, M.; Ebine, S. *Synthesis* **1981**, 472.
(12) Montserrat, N.; Parkins, A. W.; Tomkins, A. R. *J. Chem. Res., Synop.* **1995**, 336.

Table 1. Selected NMR Chemical Shifts (ppm) and Coupling Constants (Hz) of the Imidazol(in)e Heterocyclic Core N(1)−C(2)−N(3)−C(4)−C(5) and of C(1)$_{ferrocenyl}$ for Compounds 3, 4c, 5, 6, 7, 8, and 9

nucleus	3	4c	5	6	7
^{13}C [C(2)]	71.2	151.3	*a*	134.4	134.5
^{13}C [C(4,5)]	49.4	50.4	48.8	123.8	123.9
^{1}H [H(2)]	4.07	8.31	*b*	9.05	8.93
^{1}H [H(4,5)]	3.28	4.32	4.01	7.80	7.76
^{13}C [C(1)$_{ferrocenyl}$]	*a*	95.1	*a*	92.1	93.1

nucleus	8	9
^{13}C [C(2)]	*a*	180.6; $^{1}J(^{13}C-^{107}Ag) = 189$ Hz, $^{1}J(^{13}C-^{109}Ag) = 219$ Hz
^{13}C [C(4,5)]	119.2	
^{1}H [H(2)]	*b*	*c*
^{1}H [H(4,5)]	7.14	7.43; $^{4}J(^{1}H-^{107/109}Ag) = 1.6$ Hz
^{13}C [C(1)$_{ferrocenyl}$]	95.4	97.9; $^{3}J(^{13}C-^{107/109}Ag) = 1.0$ Hz

[a] Not observed. [b] Quaternary thione carbon with no ^{1}H resonance. [c] Quaternary carbene carbon with no ^{1}H resonance.

We investigated some coordination chemistry of Fc-DAB, including applications of this new bulky ligand in Ni(II) and Pd(II) complexes as precatalysts for olefin homo- and copolymerizations[14] and the redox behavior of selected transition metal carbonyl complexes.[15]

Reduction of Fc-DAB (**1**) with $LiAlH_4$ cleanly affords yellow 1,4,-diferrocenylethylene-1,2-diamine (**2**) (Scheme 2), and subsequent condensation with aqueous formaldehyde with concomitant ring closure yields 1,3-diferrocenylimidazolidine (**3**). The NMR spectra of compounds **1, 2,** and **3** show all the expected signals with the typical signal pattern of monosubstituted ferrocenyl groups. Table 1 lists some pertinent ^{1}H and ^{13}C resonances of **3** for comparison with the NMR spectral properties of the heterocyclic core of the other saturated and unsaturated imidazole compounds discussed below. Clearly evident is the saturated character of the ring system in **3** with ^{1}H and ^{13}C resonances (compare Table 1) in the aliphatic region. A single-crystal X-ray structure analysis of **3** gave further proof of the identity of **3**, showing a folded imidazolidine ring and a cisoid conformation of the two slightly twisted *N*-ferrocenyl substituents (Figure 1, Table 2).

Oxidation with trityl tetrafluoroborate or hexafluoroborate as hydride abstracting reagents[16] yields the corresponding imidazolinium salts **4a** and **4b**, respectively. Both compounds are clearly identified by their positive mode FAB mass spectra with a parent peak [$m/z = 439$(100%)] of the 1,3-diferrocenylimidazolinium cation. The single-crystal structure analysis of **4b** (Figure 2, Table 2) shows the planar N(1)−C(11)−N(1a) amidinium subunit, as expected, and, similar to the structure of the precursor **3**, a cisoid conformation of the ferrocenyl substituents. Although we could only obtain suitable single crystals for compound **4b**, the purification of both salts **4a** and **4b** on a preparative scale is difficult and most of the material was lost on attempted purification for a full characterization by spectroscopic methods. Therefore we converted **4a** by anion exchange to tetraphenylborate **4c,** which is much more soluble in common organic solvents and can be obtained in pure form with satisfactory spectroscopic properties and elemental analysis. The NMR spectroscopic data of **4c** (Table 1) show the expected upfield shift of the C(2) carbon and the H(2) hydrogen of the amidinium subunit in comparison to its neutral and

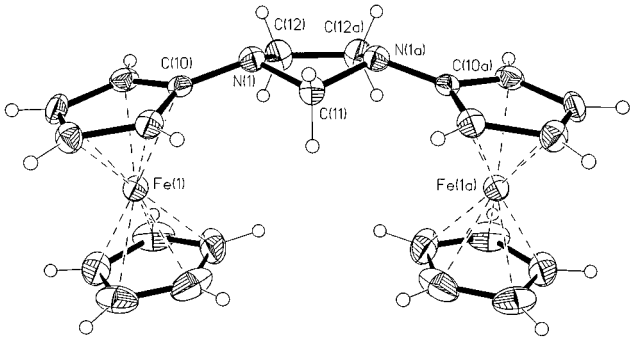

Figure 1. Molecular structure of **3**, showing the atom-numbering scheme. Cyclopentadienyl carbons of ferrocene 1 are C(1)−C(10). Selected bond distances and angles: C(11)−N(1) = 145.0(4), N(1)−C(12) = 147.4(5), C(12)−C(12a) = 151.2(8), N(1)−C(10) = 139.0(5) pm; N(1)−C(11)−N(1a) = 102.4(4), C(10)−N(1)−C(11) = 117.8(3), C(10)−N(1)−C(12) = 117.8(3), N(1)−C(12)−C(12a) = 104.7(2), tilt angle plane [C(10)−C(9)−C(8)−C(7)−C(6)] vs plane [N(1)−C(12)−C(12a)−N(1a)] = 22.7(3)°.

Table 2. Crystal Data and Structure Refinement for 3 and 4b

	3	4b
mol formula	$C_{23}H_{24}Fe_2N_2$	$C_{23}H_{23}F_6Fe_2N_2P$
fw	440.14	584.10
cryst syst	orthorhombic	orthorhombic
space group	*Pnma* (No. 62)	*Pnma* (No. 62)
a (pm)	805.4(1)	959.0(2)
b (pm)	2291.7(4)	2494.3(9)
c (pm)	999.5(1)	901.4(1)
α (deg)	90	90
β (deg)	90	90
γ (deg)	90	90
V (nm^3)	1.8448(4)	2.1562(9)
Z	4	4
temp (K)	218(2)	213(2)
d(calcd) (Mg/m^3)	1.585	1.799
abs coeff (mm^{-1})	1.583	1.487
F(000)	912	1184
color, habit	orange platelet	orange plate
cryst size (mm)	0.45 × 0.45 × 0.06	0.6 × 0.45 × 0.17
θ range for data collcn (deg)	3.25−22.99	3.10−23.49
index ranges	$0 \le h \le 8$ $-25 \le k \le 1$ $0 \le l \le 11$	$0 \le h \le 10$ $-1 \le k \le 27$ $0 \le l \le 10$
no. of rflns collcd	1359	1709
no. of indep rflns	1315 ($R_{int} = 0.0690$)	1627 ($R_{int} = 0.0164$)
no. of rflns with $I > 2\sigma(I)$	2285	1376
abs cor	Ψ-scan	Ψ-scan
max and min transm	0.969 and 0.831	1.000 and 0.695
refinement method	full-matrix least-squares on F^2	full-matrix least-squares on F^2
no. of data/restraints/params	1177/0/125	1535/0/182
goodness-of-fit on F^2	1.082	1.054
final *R* indices [$I > 2\sigma(I)$]	$R_1 = 0.0349$ $wR_2 = 0.0712$	$R_1 = 0.0289$ $wR_2 = 0.0702$
R indices (all data)	$R_1 = 0.0685$ $wR_2 = 0.1809$	$R_1 = 0.0415$ $wR_2 = 0.1266$
max diff peak/hole (e nm^{-3})	287 and −221	386 and −329

(13) Vrieze, K.; van Koten, G. *Comprehensive Coordination Chemistry*; Wilkinson, G., Gillard, R. D., McCleverty, J. A., Eds.; Pergamon: Oxford, 1987; Vol. 2, p 206.

(14) Bildstein, B.; Malaun, M.; Hradsky, A.; Gonioukh, A.; Micklitz, W. Pat. pending DE 19920486.1, 1999.

(15) Bildstein, B.; Malaun, M.; Kopacka, H.; Fontani, M.; Zanello, P. *Inorg. Chim. Acta*, submitted.

(16) Straus, D. A.; Zhang, C.; Tilley, T. D. *J. Organomet. Chem.* **1989**, *369*, 13.

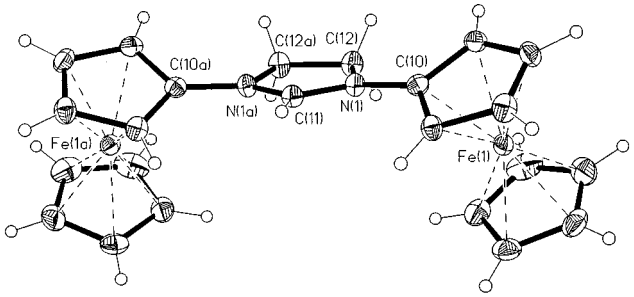

Figure 2. Molecular structure of the cation of **4b**, showing the atom-numbering scheme. Cyclopentadienyl carbons of ferrocene 1 are numbered analogously to those in the structure of **3**. Selected bond distances and angles: C(11)−N(1) = 130.4(3), N(1)−C(12) = 147.6(4), C(12)−C(12a) = 153.3(6), N(1)−C(10) = 142.0(4) pm; N(1)−C(11)−N(1a) = 113.9(3), C(10)−N(1)−C(11) = 126.0(2), C(10)−N(1)−C(12) = 123.4(2), N(1)−C(12)−C(12a) = 102.76(14), tilt angle plane [C(10)−C(9)−C(8)−C(7)−C(6)] vs plane [N(1)−C(12)−C(12a)−N(1a)−C(11)] = 29.2(2)°.

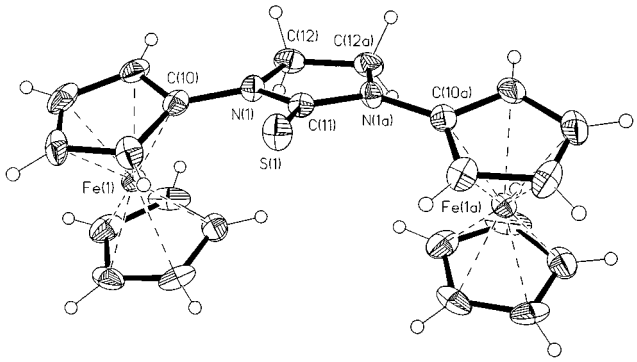

Figure 3. Molecular structure of **5**, showing the atom-numbering scheme. Cyclopentadienyl carbons of ferrocene 1 are numbered analogously to those in the structure of **3**. Selected bond distances and angles: S(1)−C(11) = 167.5(7), C(11)−N(1) = 135.6(5), N(1)−C(12) = 146.5(6), C(12)−C(12a) = 151.6(11), N(1)−C(10) = 141.7(6) pm; S(1)−C(11)−N(1) = 126.0(3), N(1)−C(11)−N(1a) = 108.0(6), C(10)−N(1)−C(11) = 128.1(4), C(10)−N(1)−C(12) = 118.9(4), N(1)−C(12)−C(12a) = 103.4(2), tilt angle plane [C(10)−C(9)−C(8)−C(7)−C(6)] vs plane [N(1)−C(12)−C(12a)−N(1a)−C(11)] = 20.3(3)°.

reduced precursor **3**. The ^{1}H and ^{13}C signals of the ferrocenyl substituents are typical for a "regular" monosubstituted ferrocene, ruling out any positive charge delocalization involving the metallocenyl groups directly bonded to the amidinium nitrogens, in contrast to all-carbon conjugated cationic systems, where the adjacent ferrocenyl substituents contribute significantly to the overall charge dispersal.[3,4]

In general, cationic *N*,*N*′-disubstituted-*N*-heterocycles serve as the key progenitors of *N*-heterocyclic carbenes.[1,2] Deprotonation of **4c** with methyllithium and subsequent trapping of the intermediate 1,3-diferrocenylimidazolin-2-ylidene with elemental sulfur affords thiourea **5** in 56% yield. Interestingly, attempting the same reaction with potassium tertiary butoxide as base in the presence of excess sulfur left all of the starting material unchanged, in contrast to the analogous reaction of *N*-ferrocenyl-*N*′-methylbenzimidazolium,[7] where a 98% conversion to the desired thiourea was observed. This indicates that imidazolinium salts are less acidic in comparison to (benz)imidazolium salts, as might have been expected, suggesting that two *N*-ferrocenyl substituents in comparison to only one *N*-ferrocenyl substituent prevent deprotonation by a sterically demanding base like KO-t-Bu, either due to steric hindrance or due to the additional donor effect of the second *N*-ferrocenyl group. An X-ray single-crystal structure (Figure 3, Table 3) of thiourea **5** shows a planar imidazoline-2-thione backbone with slightly tilted and cisoid ferrocenyl substituents; relevant bond distances and angles are given in the caption of Figure 3. The ^{1}H signals (Table 1) of the ethylene hydrogens H(4,5) of **5** are detected intermediate between those of the saturated imidazolidine **3** and the cationic imidazolinium **4c** in consonance with the acceptor properties of the thiourea functionality.

One objective of this work was the preparation of the "free" carbene 1,3-diferrocenylimidazolin-2-ylidene by deprotonation of the cationic *N*-heterocyclic precursor with a suitable base. However, all our attempts under a variety of conditions with combinations of different solvents and bases[2] met with failure, and no free carbene could be isolated upon workup under strictly anhydrous conditions. An alternative route to *N*-heterocyclic carbenes by reduction of *N*,*N*′-disubstituted thioureas with an excess of potassium in refluxing THF has been develeoped by N. Kuhn,[17] but no reaction of thiourea **5** was observed under these conditions and the

Table 3. Crystal Data and Structure Refinement for 5 and 7

	5	**7**
mol formula	$C_{23}H_{22}Fe_2N_2S$	$C_{47}H_{41}BFe_2N_2$
fw	470.19	756.33
cryst syst	orthorhombic	orthorhombic
space group	*Pnma* (No. 62)	$P2_12_12_1$ (No. 19)
a (pm)	1075.6(4)	1009.2(2)
b (pm)	2400.3(4)	1868.9(2)
c (pm)	740.5(1)	1932.9(2)
α (deg)	90	90
β (deg)	90	90
γ (deg)	90	90
V (nm^3)	1.9118(8)	3.6456(9)
Z	4	4
temp (K)	293(2)	213(2)
d(calcd) (Mg/m^3)	1.634	1.378
abs coeff (mm^{-1})	1.638	0.833
F(000)	968	1576
color, habit	red prism	yellow prism
cryst size (mm)	0.4 × 0.35 × 0.20	0.9 × 0.3 × 0.25
θ range for data collcn (deg)	2.88−22.49	2.52−23.00
index ranges	$-1 \le h \le 11$ $-1 \le k \le 25$ $-1 \le l \le 7$	$-1 \le h \le 11$ $-1 \le k \le 20$ $-1 \le l \le 21$
no. of rflns collcd	1783	3649
no. of indep rflns	1278 (R_{int} = 0.0428)	3450 (R_{int} = 0.0136)
no. of rflns with $I > 2\sigma(I)$	942	3017
abs cor	Ψ-scan	Ψ-scan
max and min transm	0.966 and 0.693	0.942 and 0.898
refinement method	full-matrix least-squares on F^2	full-matrix least-squares on F^2
no. of data/restraints/params	1173/0/131	3350/0/470
goodness-of-fit on F^2	1.068	1.061
final *R* indices [$I > 2\sigma(I)$]	R_1 = 0.0410 wR_2 = 0.0978	R_1 = 0.0306 wR_2 = 0.0565
R indices (all data)	R_1 = 0.0665 wR_2 = 0.1119	R_1 = 0.0424 wR_2 = 0.0621
max diff peak/hole (e nm^{-3})	429 and −404	220 and −234

(17) Kuhn, N. *Synthesis* **1993**, 561.

Scheme 3. Synthesis of Compounds 6−9 (Fc = ferrocenyl)

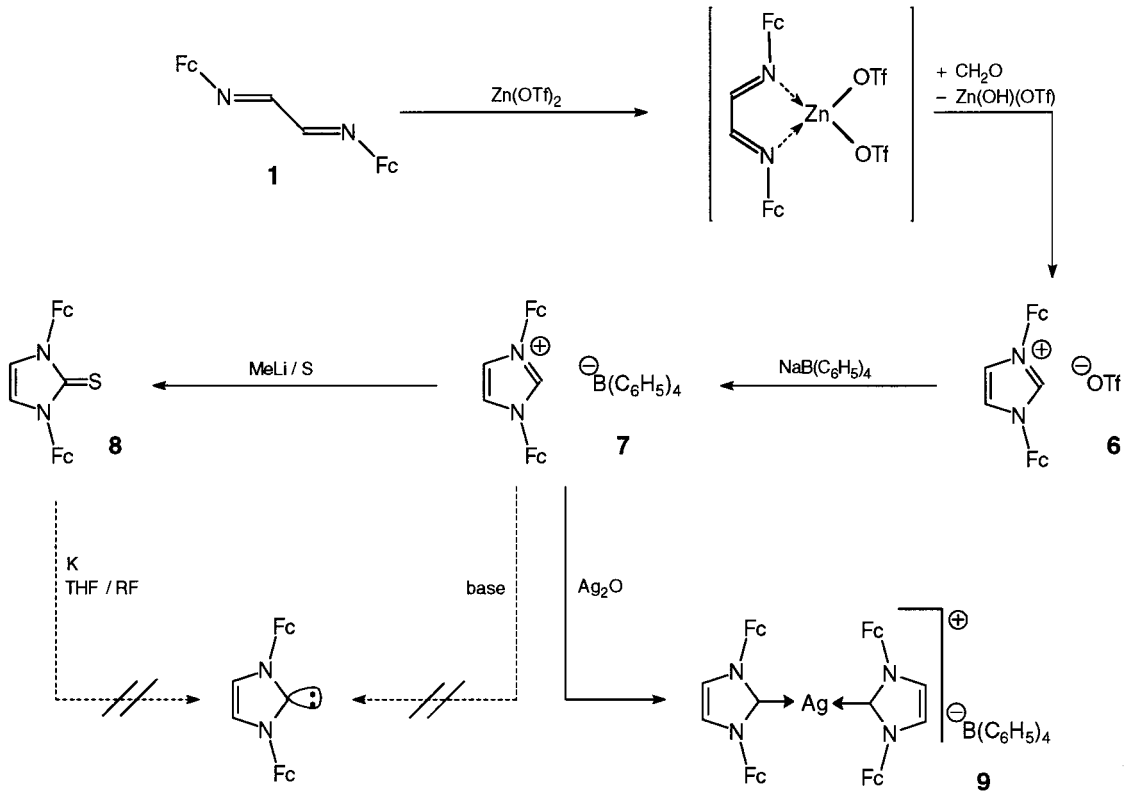

starting material was recovered in quantitative yield after a reaction period of 48 h. Whereas in the generation of the carbene by attempted removal of the formamidinium proton from **4c** by interaction with a base steric hindrance might be responsible for the negative result, in the attempted reduction of thiourea **5** with potassium no such steric hindrance can be envisaged, suggesting mainly electronic reasons for the limited stability or inaccessibility of the free carbene 1,3-diferrocenylimidazolin-2-ylidene.

Metal complexes of nucleophilic *N*-heterocyclic carbenes can in general be prepared either by ligand exchange reactions of the free carbenes with metal complexes or by an in situ deprotonation of the azolium precursor in the presence of the metal complex.[2] We have shown earlier[6,7] that such reactions are indeed possible with alkyl-spacered or directly *N*-linked substituted ferrocenyl benzimidazolium compounds, affording Hg(II) and Pd(II) complexes in analogy with other non-ferrocenylated azolium precursors.[2] Recently also Ag(I) carbene complexes have been prepared by an in situ deprotonation/complexation reaction using Ag_2O.[18] Consequently it was of prime interest if 1,3-diferrocenylimidazolinium salts **4** can be used for the synthesis of metal carbene derivatives. Unfortunately, this is not the case. Attempted preparation of Ag(I), Hg(II), or Pd(II) complexes (Scheme 2) by reaction of **4c** with the corresponding metal salts Ag_2O, $Hg(OAc)_2$, or $Pd(OAc)_2$, respectively, did not afford the desired products. Again, one might reason that steric hindrance prevented deprotonation and/or complex formation, but in the light of the successful preparation of Ag(I) complex **9** (see below) we believe that mainly the reduced acidity of the 1,3-diferrocenylimidazolinium salts is responsible for the unobserved reactivity, indicating that acetate or oxide, respectively, are too weak bases to deprotonate 1,3-diferrocenylimidazolinium salts.

In summary, *N,N′*-diferrocenylimidazolin-2-ylidenes cannot be prepared as the free carbenes nor can the imidazolinium precursors be converted to metal derivatives by in situ deprotonation and complex formation under standard[2] reaction conditions.

Synthesis and Properties of 1,3-Diferrocenylimidazole Compounds. Diferrocenyldiazabutadiene (Fc-DAB, **1**) is also the starting material for the synthesis of 1,3-diferrocenylimidazole compounds (Scheme 3), as noted above. Recently it was shown by A. L. Spek, G. van Koten, and co-workers[19] that *N,N′*-disubstituted imidazolium salts can be synthesized by reaction of a $Zn(R\text{-}DAB)(OTf)_2$ complex with paraformaldehyde, involving (i) activation of the DAB ligand by complex formation with the strong Lewis acid zinc ditriflate (prepared in situ from diethylzinc and triflic acid), (ii) coordination of formaldehyde via its oxygen lone pair to an intermediate monodentate DAB Zn complex, (iii) intramolecular nucleophilic attack of the formaldehyde carbonyl by the free nitrogen of the monodentate-coordinated DAB ligand, and (iv) rearrangement with concomitant ring closure and elimination of zinc hydroxide triflate Zn(OH)(OTf).

Applying these new reaction conditions to Fc-DAB did indeed afford the desired 1,3-diferrocenylimidazolium triflate **6**, albeit in a mediocre yield of only 30% (Scheme 3). In addition, we note that the standard synthesis of imidazolium salts[8] failed completely in the case of

(18) Wang, H. M. J.; Lin, I. J. B. *Organometallics* **1998**, *17*, 972.

(19) Rijnberg, E.; Richter, B.; Thiele, K.-H.; Boersma, J.; Veldman, N.; Spek, A. L.; van Koten, G. *Inorg. Chem.* **1998**, *37*, 56.

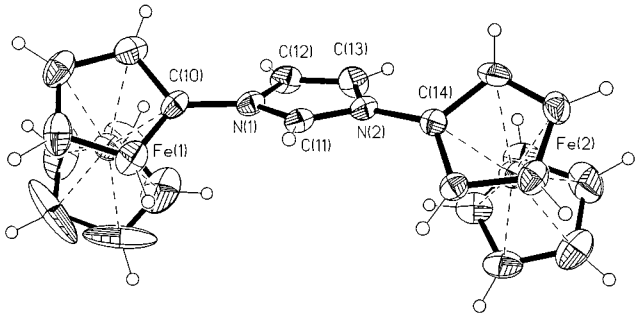

Figure 4. Molecular structure of the cation of **7**, showing the atom-numbering scheme. Cyclopentadienyl carbons of ferrocene 1 are C(1)−C(10) and of ferrocene 2 C(14)−C(23), respectively. Selected bond distances and angles: C(11)−N(1) = 133.4(5), N(1)−C(12) = 137.6(5), C(12)−C(13) = 133.1(6), C(13)−N(2) = 138.0(5), N(2)−C(11) = 132.5(5), N(1)−C(10) = 142.4(5), N(2)−C(14) = 143.8(5) pm; N(1)−C(11)−N(2) = 108.4(4), C(10)−N(1)−C(11) = 125.5(4), C(10)−N(1)−C(12) = 126.0(4), N(1)−C(12)−C(13) = 107.6(4), C(12)−C(13)−N(2) = 107.3(4), C(14)−N(2)−C(11) = 125.6(4), C(14)−N(2)−C(13) = 125.8(4), tilt angle plane [C(10)−C(9)−C(8)−C(7)−C(6)] vs plane [N(1)−C(12)−C(13)−N(2)−C(11)] = 38.2(2), tilt angle plane [C(14)−C(15)−C(16)−C(17)−C(18)] vs plane [N(2)−C(13)−C(12)−N(1)−C(11)] = 40.9(2)°.

aminoferrocene. For further reactions, mainly to increase the solubility of the azolium precursor, triflate **6** was converted in 52% yield to tetraphenylborate **7** by anion exchange with sodium tetraphenylborate in methanolic solution. Imidazolium salts **6** and **7** show spectroscopic properties (Table 1) which compare as anticipated with those of their saturated analogue **4c**: the aromatic delocalization in **6** or **7** results in (i) shielded ^{13}C resonances of carbon C(2) in comparison to the amidinium carbon of **4c**, (ii) deshielded ^{13}C signals of the aromatic carbons C(4,5) in comparison to the corresponding aliphatic carbons of **4c**, and (iii) corresponding low-field-shifted ^{1}H signals H(4,5) as compared to the aliphatic resonances H(4,5) of **4c**. The NMR spectral properties of the two ferrocenyl substituents of **6** or **7** show the typical pattern of regular monosubstituted ferrocenes, indicating no unusal charge distribution involving the adjacent metallocenyl moieties. The single-crystal structure of **7** (Figure 4, Table 3) confirms these structural assignments; the cation of **7** has a planar imidazole backbone with slightly twisted cisoid *N*-ferrocenyl substituents.

Thiourea **8** is synthesized by deprotonation with methyllithium and sequential trapping of the intermediate 1,3-diferrocenylimidazol-2-ylidene with elemental sulfur. The NMR properties of **8** are as anticipated (Table 1), and the solid-state structure (Figure 5, Table 4) gives further proof of the identity of **8**, showing a planar imidazole-2-thione with cisoid *N*-ferrocenyl groups. The main reason for the preparation of **8** was its possible use as a progenitor of the free carbene 1,3-diferrocenylimidazol-2-ylidene by reduction with potassium in boiling THF according to Kuhn's procedure.[17] However, no clean reaction occurred, and the starting thiourea was consumed without any positive outcome in terms of an isolable product. Similarly, attempted deprotonation of imidazolium salt **7** with different bases[2] according to Scheme 3 did not allow the synthesis of 1,3-diferrocenylimidazol-2-ylidene in a practical manner.

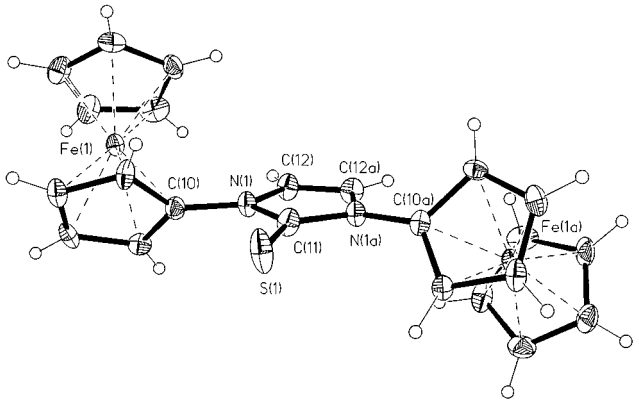

Figure 5. Molecular structure of **8**, showing the atom-numbering scheme. Cyclopentadienyl carbons of ferrocene 1 are numbered analogously to those in the structure of **3**. Selected bond distances and angles: S(1)−C(11) = 167.1(11), C(11)−N(1) = 137.9(9), N(1)−C(12) = 140.2(10), C(12)−C(12a) = 133(2), N(1)−C(10) = 141.5(10) pm; S(1)−C(11)−N(1) = 127.7(5), N(1)−C(11)−N(1a) = 104.6(9), C(10)−N(1)−C(11) = 124.9(7), C(10)−N(1)−C(12) = 124.9(6), N(1)−C(12)−C(12a) = 107.6(4), tilt angle plane [C(10)−C(9)−C(8)−C(7)−C(6)] vs plane [N(1)−C(12)−C(12a)−N(1a)−C(11)] = 53.7(3)°.

Table 4. Crystal Data and Structure Refinement for 8 and 9

	8	**9**
mol formula	$C_{23}H_{20}Fe_2N_2SH$	$C_{70}H_{60}AgBFe_4N_4$• 0.5 $CHCl_3$•1.5 MeO
fw	468.17	1407.05
cryst syst	monoclinic	triclinic
space group	*C*2/*c* (No. 15)	*P*$\bar{1}$(No. 2)
a (pm)	2674.0(5)	1385.4(2)
b (pm)	739.0(2)	1464.6(2)
c (pm)	1050.3(3)	1756.3(1)
α (deg)	90	92.23(1)
β (deg)	112.59(2)	110.54(1)
γ (deg)	90	104.350(10)
V (nm^3)	1.9162(8)	3.2017(7)
Z	4	2
temp (K)	213(2)	213(2)
d(calcd) (Mg/m^3)	1.623	1.460
abs coeff (mm^{-1})	1.634	1.296
F (000)	960	1440
color, habit	yellow prism	yellow prism
cryst size (mm)	0.35 × 0.3 × 0.05	0.7 × 0.3 × 0.22
θ range for data collcn (deg)	2.88−22.00	2.50−23.50
index ranges	$-1 \le h \le 28$ $-1 \le k \le 7$ $-11 \le l \le 11$	$0 \le h \le 14$ $-16 \le k \le 15$ $-19 \le l \le 18$
no. of rflns collcd	1400	9667
no. of indep rflns	1141 (R_{int} = 0.0542)	9232 (R_{int} = 0.0133)
no. of rflns with $I > 2\sigma(I)$	864	7717
abs cor	Ψ-scan	Ψ-scan
max and min transm	1.000 and 0.741	0.942 and 0.898
refinement method	full-matrix least-squares on F^2	full-matrix least-squares on F^2
no. of data/restraints/params	918/0/128	8763/1/782
goodness-of-fit on F^2	1.083	1.039
final *R* indices [$I > 2\sigma(I)$]	R_1 = 0.0588	R_1 = 0.0393
	wR_2 = 0.1460	wR_2 = 0.1028
R indices (all data)	R_1 = 0.1319	R_1 = 0.0516
	wR_2 = 0.5098	wR_2 = 0.1237
max diff peak/hole (e nm^{-3})	723 and −420	881 and −399

Therefore we turned our attention to the use of imidazolium salt **8** as a precursor for carbene derivatives by in situ deprotonation and complexation reactions. And indeed, interaction of **8** with Ag_2O affords silver(I)

complex **9** in 63% yield (Scheme 3) as a yellow air-stable material, following recently published procedures.[18] Complex **9** is fully characterized by a number of analytical techniques: High-resolution positive mode mass spectroscopy with electrospray ionization gave the parent peak of the cation $m/z = 978.9713$, in good concordance with the calculated value $m/z = 978.9700$. Multinuclear NMR spectroscopy shows very well resolved spectra with the expected number of signals and with heteronuclear couplings between ^{1}H, ^{13}C, ^{107}Ag, ^{109}Ag, ^{10}B, ^{11}B (Table 1, Experimental Section). Noteworthy are the ^{13}C chemical shifts and silver couplings of the (i) carbene carbon ($\delta = 180.6$ ppm, d × d, $^{1}J(^{13}C-^{107}Ag) = 189$ Hz, $^{1}J(^{13}C-^{109}Ag) = 219$ Hz), in consonance with values in two other analogous silver complexes reported by Arduengo[20] ($\delta = 183.6$ ppm, d × d, $^{1}J(^{13}C-^{107}Ag) = 188$ Hz, $^{1}J(^{13}C-^{109}Ag) = 209$ Hz) and by Lin[18] ($\delta = 188$ ppm, d × d, $^{1}J(^{13}C-^{107}Ag) = 180$ Hz, $^{1}J(^{13}C-^{109}Ag) = 204$ Hz); (ii) 4,5-imidazole carbons ($\delta = 123.4$ ppm, d, $^{3}J(^{13}C-^{107/109}Ag) = 5.7$ Hz), similar to the value reported by Arduengo[20] ($\delta = 124.2$ ppm, d, $^{3}J(^{13}C-^{107/109}Ag) = 5.4$ Hz); and (iii) 1-ferrocenyl carbons ($\delta = 95.4$ ppm, d, $^{3}J(^{13}C-^{107/109}Ag) = 1.0$ Hz). The *N*-ferrocenyl substituents appear as regular monosubstituted ferrocenes with no unusual features (except for the $^{3}J(^{13}C-^{107/109}Ag)$ coupling), similar to the cations **4c** and **7**. The ^{1}H NMR signal of the 4,5-imidazole hydrogens is detected at $\delta = 7.43$ ppm with a resolved coupling to silver (d, $^{4}J(^{1}H-^{107/109}Ag) = 1.6$ Hz), almost identical to the values reported by Arduengo[20] ($\delta = 7.45$ ppm, d, $^{4}J(^{1}H-^{107/109}Ag) = 1.5$ Hz). Using this $^{4}J(^{1}H-^{107/109}Ag)$ coupling in an INEPT experiment allows easy detection of the ^{109}Ag chemical shift of **9** ($\delta(^{109}Ag) = 727$ ppm vs 5 M aqueous silver nitrate), but the expected quintet ($^{4}J(^{1}H-^{107/109}Ag) = 1.6$ Hz) was not resolved due to chemical shift anisotropy. Interestingly, this ^{109}Ag chemical shift of **9** is 84 ppm *downfield* of the value in Arduengo's complex[20] ($\delta(^{109}Ag) = 642.4$ ppm vs 5 M aqueous silver nitrate), although one might expect a high-field shift due to an increased electron density (diamagnetic shielding σ_{dia}) at the Ag center of **9** induced by the four peripheral *N*-ferrocenyl donor groups. We tentatively attribute this downfield shift to paramagnetic shielding σ_{para}, which largely determines the chemical shift of transition metals in general and whose sign is opposite of σ_{dia}. Unfortunately, no further comparable ^{109}Ag chemical shifts are available in the literature.

A single-crystal structure analysis shows the complex **9** to consist of a nearly linear (C(1)−Ag(1)−C(4) = 176.8(2)°) L−Ag−L cation (L = 1,3-diferrocenylimidazol-2-ylidene) (Figure 6, Table 2) and a tetrahedral $B(C_6H_5)_4$ anion (not shown in Figure 6). The bond distances of Ag(I) to the two carbene carbons are 208.2(4) and 209.2(4) pm, similar to reported values in other L−Ag−L complexes,[18,20] with an interplanar angle of 38.4(2)° between the two imidazol-2-ylidene ligands. All the ferrocenyl substituents are twisted with respect to these imidazol-2-ylidene ligands, with angles ranging from 26.8(3)° to 51.4(2)°. One pair of ferrocenyl substituents shows a transoid conformation (Fe 1 and Fe 2), whereas the other pair is cisoid (Fe 3 and Fe 4). In comparison

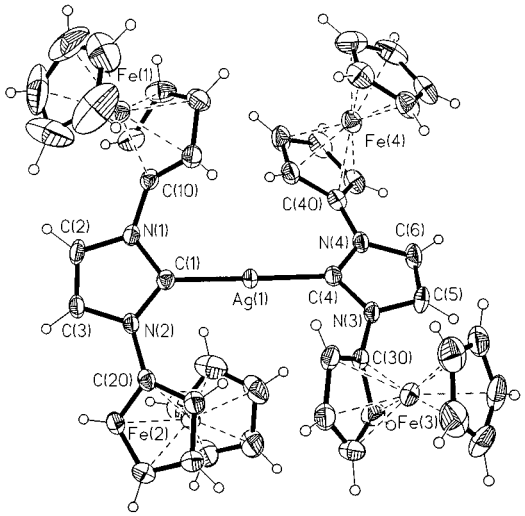

Figure 6. Molecular structure of the cation of **9**, showing the atom-numbering scheme. Solvent molecules ($CHCl_3$ and H_3COH) are omitted for clarity. Cyclopentadienyl carbons of ferrocenes 1, 2, 3, and 4 are C(10)−C(19), C(20)−C(29), C(30)−C39), and C(40)−C(49), respectively. Selected bond distances and angles: Ag(1)−C(1) = 208.2(4), Ag(1)−C(4) = 209.2(4), C(1)−N(1) = 136.4(5), C(1)−N(2) = 135.4(5), N(1)−C(2) = 138.8(5), N(1)−C(10) = 142.1(5), C(2)−C(3) = 132.2(6), N(2)−C(3) = 139.1(5), N(2)−C(20) = 142.4(5), C(4)−N(3) = 136.9(5), C(4)−N(4) = 135.0(5), N(3)−C(30) = 141.8(5), N(3)−C(5) = 139.6(5), C(5)−C(6) = 132.6(7), N(4)−C(40) = 143.0(5), N(4)−C(6) = 138.8(5) pm; C(1)−Ag(1)−C(4) = 176.8(2), Ag(1)−C(1)−N(1) = 126.7(3), Ag(1)−C(1)−N(2) = 129.1(3), Ag(1)−C(4)−N(3) = 125.5(3), Ag(1)−C(4)−N(4) = 130.4(3), N(1)−C(1)−N(2) = 103.8(3), N(3)−C(4)−N(4) = 104.1(3), tilt angle plane [C(1)−N(1)−C(2)−C(3)−N(2)] vs plane [C(4)−N(3)-C(5)−C(6)−N(4) = 38.4(2), tilt angle plane [C(10)−C(11)−C(12)−C(13)−C(14)] vs plane [N(1)−C(1)−N(2)−C(3)−C(2)] = 45.5(2), tilt angle plane [C(20)−C(21)−C(22)−C(23)−C(24)] vs plane [N(1)−C(1)−N(2)−C(3)−C(2)] = 27.8(2), tilt angle plane [C(30)−C(31)−C(32)−C(33)−C(34)] vs plane [N(3)−C(4)−N(4)−C(6)−C(5)] = 51.4(2), tilt angle plane [C(40)−C(41)−C(42)−C(43)−C(44)] vs plane [N(3)−C(4)−N(4)−C(6)−C(5)] = 26.8(3)°.

to the other structures discussed above, these various twist angles and cisoid or transoid orientations of the ferrocenyl groups indicate that mainly crystal packing forces are responsible for the observed conformations in all these structures.

The main feature of the X-ray crystal structure of **9**, as noted above, is the anticipated linear coordination of Ag^{+} with two identical carbene ligands, thereby forming a homoleptic two-coordinate linear cationic L−Ag−L complex.

Raman spectroscopy on single crystals of **9** allowed the detection of a band at 70 cm^{-1}, which we assign to a symmetric L−Ag−L stretching vibration (L = 1,3-diferrocenylimidazol-2-ylidene). To our knowledge, this is the first time that a nucleophilic carbene metal complex has been investigated by Raman spectroscopy. The general chemical similarity of nucleophilic carbenes with phosphines has been pointed out in the literature,[2] and it is interesting to note that the linear two-coordinate trimesitylphosphine Ag^{+} complex[21] (R_3P)−

(20) Arduengo, A. J., III; Dias, H. V. R.; Calabrese, J. C.; Davidson, F. *Organometallics* **1993**, *12*, 3405.

(21) Alyea, E. C.; Dias, S. A.; Stevens, S. *Inorg. Chim. Acta* **1980**, *44*, L203.

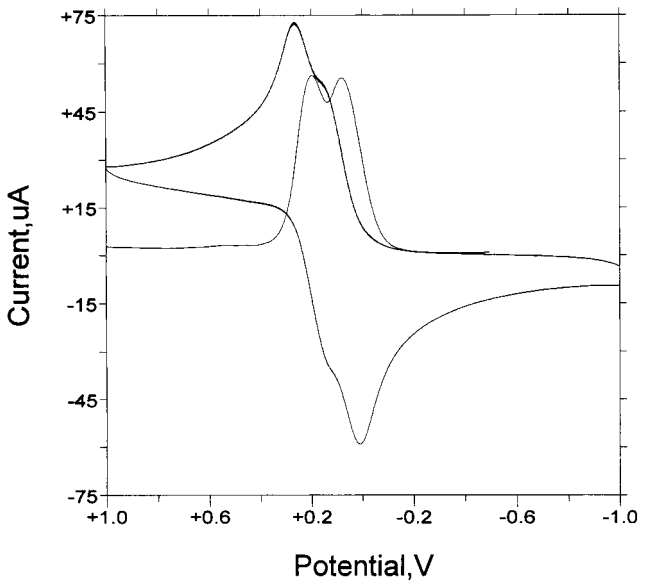

Figure 7. Cyclic and differential pulse voltammograms recorded at a platinum electrode on a CH_2Cl_2 solution containing **3** (1.7×10^{-3} mol dm^{-3}) and $N(Bu)_4PF_6$ (0.2×10^{-3} mol dm^{-3}). Scan rates: cyclic voltammogram, 0.1 V s^{-1}; DPV, 0.02 V s^{-1}.

$Ag-(PR_3)^+PF_6^-$ shows a comparable low-frequency Raman vibration at 130 cm^{-1}.

From the combined spectroscopic and structural results we conclude that **9** is electronically very similar to other nucleophilic carbene $L-Ag^+-L$ complexes,[18,20] and therefore the *N*-ferrocenyl substituents have no unusual electronic effect on the properties of such carbene complexes in general. Hence one would expect that also other carbene complexes of the 1,3-diferrocenylimidazol-2-ylidene ligand can be synthesized starting from **9** as carbene transfer reagent in analogy with published work by Lin.[18] However, attempted preparation of Au(I) or Pd(II) complexes by reaction of **9** with Au(CO)Cl or $PdCl_2$, respectively, failed. Similarly, the reaction of imidazolium salt **7** with transition metal acetates $Pd(OAc)_2$ or $Hg(OAc)_2$ under standard reaction conditions[2,6,7] afforded no corresponding Pd(II) or Hg(II) complexes. The lack of reaction in these attempted in situ carbene metal complex syntheses is due to steric hindrance by the two pairs of *N*,*N*′-ferrocenyl substituents in the case of **9** and reduced acidity of imidazolium salt **7**, preventing its deprotonation with the weak base acetate.

Electrochemistry. Figure 7 illustrates the redox ability of complex **3** through its cyclic and differential pulse voltammetric responses in dichloromethane solution. As expected, the diferrocenyl complex undergoes two oxidation steps, which are almost overlapped in cyclic voltammetry, but sufficiently well separated in differential pulse voltammetry. Controlled potential coulometry in correspondence to the most anodic process ($E_w = +0.6$ V) consumes two electrons/molecule. Cyclic voltammetric tests performed on the solution resulting from exhaustive oxidation display profiles quite complementary to the original ones, indicating chemical reversibility of the overall redox change **3**/**3**$^{2+}$. In contrast to the usually observed blue-to-green color of ferrocenium species in which the HOMO is essentially contributed by the d orbitals of the central iron,[22] in the case of **3**$^{2+}$ an orange solution is obtained, suggesting significant participation of the imidazoline orbitals with the HOMO of the molecule. The small separation between the two one-electron oxidations ($E^{\circ\prime} = 0.12$ V) indicates some minor electronic communication between the two ferrocenyl fragments with a K_{com} value of about 10^2, ruling out a substantially valence-trapped, class I mixed-valent monocation **3**$^+$.

Table 5. Formal Electrode Potential Values (in V, vs SCE) and Relevant Separations (in mV) for the Sequential One-Electron Oxidations of the Diferrocenyl Compounds 3, 4c, 5, 7, and 8 in Dichloromethane Solution

compound	$E^{\circ\prime}$ (first oxidation)	$E^{\circ\prime}$ (second oxidation)	$\Delta E^{\circ\prime}$	K_{com}
3	+0.09	+0.21	116	91
4c	+0.53	+0.65	120	107
7	+0.75	+0.75	*a*	
5	+0.31	+0.43	126	135
8	+0.46	+0.55	90	33
$Fe(C_5H_5)_2$	+0.38			

[a] Not verifiable.

Thioureas **5** and **8** exhibit voltammetric responses qualitatively similar to those of **3** (Table 5). However, electrogenerated dications **5**$^{2+}$ and **8**$^{2+}$ proved to be less stable in comparison to **3**$^{2+}$, as indicated by reduction currents about one-half of those relevant to the original oxidation processes. The two oxidation processes of **5** and **8** are shifted toward positive potential values versus those of **3** (**5**, 0.2 V; **8**, 0.15 V), explainable by the electron-withdrawing thiocarbonyl moiety and the increased unsaturation in the case of **8**, but somewhat surprisingly no substantial variation in the communication between the two ferrocenyl groups is observed for compounds **3**, **5**, and **8**.

To account for the electrochemical behavior of the cationic species **4c** and **7**, it is necessary to state that the tetraphenylborate anion itself is redox active, giving rise to an irreversible oxidation in the region from +0.7 to +0.8 V, depending on concentration and scan rates. In the case of complex **4c**, the appearance of the previous two close-spaced oxidations is easily detected, even if the closeness of the subsequent anodic oxidation of the $B(C_6H_5)_4$ counteranion prevented reliable coulometric measurements on the stability of the corresponding trication. In contrast, the voltammetric profile of **7**, either in cyclic or differential pulse voltammetry, is quite overlapped by the tetraphenylborate oxidation, preventing the ascertainment of the oxidation taking place through a single two-electron or two close one-electron steps. As Table 5 shows, the oxidation of the cationic species **4c** and **7** occurs at potentials notably more positive than those of **3**, attributable to the increasing unsaturation of the imidazole ring and/or coulomb effects. Even if not unexpected, it is interesting to note that a few related benzimidazole-*N*-ferrocenylalkyl derivatives display a single two-electron oxidation.[6] This result points out that the imidazole or benzimidazole moieties allow in principle electron flow within multimetallic assemblies.

Finally, we examined the electrochemical behavior of the tetraferrocenyl silver(I) monocation **9**. Also in this

(22) Sohn, Y. S.; Hendrickson, D. N.; Gray, H. B. *J. Am. Chem. Soc.* **1971**, *93*, 3603.

case the presence of the $B(C_6H_5)_4$ counteranion interfered with an accurate analysis of the voltammetric responses. Either in cyclic or differential pulse voltammetry a single peak appeared preceding a very close shoulder at $E_p = +0.7$ V (see Figure 8 in the Supporting Information). After the consumption of four electrons/molecule in exhaustive electrolysis ($E_w = +0.8$ V), the current abruptly decayed but remained higher than the background current for long times, likely due to adsorption phenomena (which are well visible in the cyclic voltammetric profile, Figure 8). In agreement with the expected effect of the central silver(I) atom to prevent any communication between the two diferrocenyl subunits, we confidently assume the occurrence of a single four-electron oxidation. Following the decreased unsaturation, such four-electron oxidation occurs at potentials less positive by about 0.15 V with respect to the two-electron oxidation of the precursor **7**.

Summary and Conclusions

N,N′-Diferrocenyl-substituted saturated and unsaturated imidazolium salts and thioureas have been prepared starting from *N,N′*-diferrocenyldiazabutadiene. The corresponding free carbenes *N,N′*-diferrocenylimidazolin-2-ylidene and *N,N′*-diferrocenylimidazol-2-ylidene, respectively, could not be synthesized from these *N*-heterocyclic nucleophilic carbene precursors, either due to reduced acidity and/or steric hindrance in the case of the imidazol(in)ium salts or due to no reaction or decomposition upon attempted reduction of the saturated or unsaturated heterocyclic thioureas. In contrast, reaction of *N,N′*-diferrocenylimidazolium salts with Ag_2O yielded the expected silver(I) complex, which was fully characterized by a number of techniques, including IR, single-crystal Raman, HRMS, ^{1}H, ^{13}C, and ^{109}Ag NMR, and X-ray structure analysis. Electrochemical measurements have shown that these *N,N′*-diferrocenyl-*N*-heterocyclic compounds oxidize through two rather close one-electron steps, indicating minor electronic communication between the two metallocenyl redox centers.

Experimental Section

General Procedures. Reactions of air-sensitive materials were carried out using standard Schlenk techniques and vacuum-line manipulations. Solvents were carefully deoxygenated, purified, and dried prior to use. *Electrochemistry:* Materials and apparatus for electrochemical measurements have been described elsewhere.[23] Differential pulse voltammograms were recorded at a BAS 100 W electrochemical analyzer under a pulse amplitude of 50 mV. All the potential values are referred to the saturated calomel electrode (SCE). *Raman Spectroscopy:* Raman spectra were recorded on a DILOR-LABRAM-I confocal microscope laser system using a 18 mW diode laser at 785 nm. *Mass Spectroscopy:* The positive mode FAB spectra (20 kV, 2 μA; matrix, *m*-nitrobenzyl alcohol) or ESI spectra (20 μl/min, 5 μL loop injection; acetonitrile or DMF/methanol, 1:1) were obtained on a Finnigan MAT95 spectrometer. Routine EI mass spectra (70 eV) were measured on a modified computer-interfaced Varian CH7 spectrometer. *NMR Spectroscopy:* The ^{1}H, ^{13}C, and ^{109}Ag NMR spectra were recorded on a Bruker DPX 300 spectrometer with signals referenced to residual solvent peaks (^{1}H) or solvent peaks (^{13}C) as internal standards and 5 M aqueous $AgNO_3$ (^{109}Ag) as external standards, respectively. The ^{109}Ag INEPT spectra were obtained with the standard INEPT sequence.[24] *Single-Crystal X-ray Structure Determinations:* X-ray crystallographic data (Table 2) were collected by a Siemens P4 diffractometer with graphite-monochromatized Mo Kα radiadtion ($\lambda = 71.073$ pm). The unit cell parameters were determined from 25 randomly selected reflections, obtained by P4 automatic routines. Data were measured via ω-scan and corrected for Lorentz and polarization effects, and an empirical absorption correction, based on ψ-scans, was applied. The structures were solved by direct methods (SHELXS-86)[25] and refined by a full-matrix least-squares procedure using F^2 (SHELXL-93).[26] The function minimized was $\sum[w(F_o^2 - F_c^2)^2]$ with the weight defined as $w^{-1} = [\sigma^2(F_o^2) + (xP)^2 + yP]$ and $P = (F_o^2 + 2F_c^2)/3$. All non-hydrogen atoms were refined with anisotropic displacement parameters. Hydrogen atoms were located by difference Fourier methods, but in the refinement they were included in calculated positions and refined with isotropic displacement parameters 1.2 times and 1.5 (for methyl hydrogen atoms) higher than U(eq) of the attached atoms. The absolute structure parameter of **7** is $-0.02(2)$. Further details of the crystal structure investigations of compounds **3**, **4b**, **5**, **7**, **8**, and **9** are available in the Supporting Information via the Internet or from the Cambridge Crystallographic Data Centre, 12 Union Road, Cambridge, CB2 1EZ, UK, on quoting the full journal citation.

Lithioferrocene (CA #1271-15-4). Modified[27] and optimized[28] procedure. *Caution: Solid dry lithioferrocene is an extremely air-sensitive pyrophoric material; therefore special precautions should be taken when performing this preparation on a large scale as described below and when transferring the product; experience in handling very air-sensitive materials is highly recommended.* A 1 L Schlenk flask equipped with a large stirring bar was charged under an atmosphere of Ar with 40 g (0.215 mol) of ferrocene and 250 mL of dry THF, and the solution was cooled in an ice bath to 0 °C; some dissolved ferrocene precipitated during this process. Under efficient stirring 165 mL of a 1.5 M *n*-hexane solution of t-BuLi (0.247 mol) was added during a period of 15 min, and immediatly after the addition was completed, 300 mL of *n*-hexane was added and the mixture was cooled to −80 °C to precipitate the crude product, consisting of a mixture of lithioferrocene and unreacted ferrocene (note: longer reaction periods decrease the yield of product). The precipitate was isolated by Schlenk filtration and washed with approximately 5 portions of 100 mL of *n*-hexane until the filtrate was almost colorless, indicating complete removal of unreacted ferrocene (note: care has to be taken not to hydrolyze the product during these operations due to the introduction of moisture and/or air). The Schlenk filter tube was evacuated, and the product was thoroughly dried in vacuo, affording a *pyrophoric* yellowish powder, which was transferred under proper precautions with protection from air to a storage Schlenk vessel, yielding 31.84 g (0.166 mol, 77.14%) of solid lithioferrocene. This material can be stored in a freezer for months with only marginal loss of activity in further reactions. Due to the extreme air-sensitivity, no analytical or spectroscopic data can be obtained for lithioferrocene.

Bromoferrocene (CA #1273-73-0). This procedure is a direct conversion of lithioferrocene to bromoferrocene, avoiding the necessity to synthesize ferrocene boronic acid[10] or toxic

(23) Zanello, P.; Laschi, F.; Fontani, M.; Mealli, C.; Ienco, A.; Tang, K.; Jin, X.; Li, L. *J. Chem. Soc., Dalton Trans.* **1999**, 965.

(24) Morris, G. A.; Freeman, R. *J. Am. Chem. Soc.* **1979**, *101*, 760.

(25) Sheldrick, G. M. *SHELXS-86: Program for Crystal Structure Solutions*; University of Göttingen: Göttingen, Germany, 1986.

(26) Sheldrick, G. M. *SHELXL-93: Program for the Refinement of Crystal Structures*; University of Göttingen: Göttingen, Germany, 1993.

(27) Guillaneux, D.; Kagan, H. B. *J. Org. Chem.* **1995**, *60*, 2502.

(28) Schottenberger, H.; Buchmeiser, M.; Polin, J.; Schwarzhans, K.-E. *Z. Naturforsch.* **1993**, *48b*, 1524.

chloromercurioferrocene[29] as precursors of bromoferrocene. A 500 mL Schlenk vessel was charged under an atmosphere of Ar with 11.12 g (0.058 mol) of lithioferrocene and 300 mL of THF at a temperature of −80 °C. Separately, a −80 °C cold solution of 3 mL (58 mmol) of Br_2 in 100 mL of THF was prepared (*caution, very exothermic reaction!)* and added dropwise during a period of 30 min to the cold suspension of lithioferrocene in THF. The cooling bath was removed, and the stirred mixture was allowed to warm to room temperature. Workup: the mixture was diluted with 300 mL of ether, the organic layer was washed with aqueous $Na_2S_2O_3$ solution and with H_2O and dried with Na_2SO_4, and the solvents were removed on a rotary evaporator, yielding a brown oil, which was filtered through a short column of Al_2O_3. The product was eluted with *n*-hexane, affording 10.19 g (38.5 mmol, 66.4%) of bromoferrocene as orange-yellow crystals, mp 28−30 °C (mp 30−32 °C).[29] This product contains minor amounts (<5%) of ferrocene and biferrocene according to TLC and NMR analysis. Further purification by chromatography is possible but unnecessary for the use of bromoferrocene as a synthon in further reactions.

Iodoferrocene (CA #1273-76-3). This procedure is a direct conversion of lithioferrocene to iodoferrocene, avoiding the necessity to synthesize (tri-*n*-butylstannyl)ferrocene[27] or ferrocene boronic acid[30] as precursors of iodoferrocene. A stirred suspension of 22.313 g (0.116 mol) of lithioferrocene in 200 mL of THF was cooled to −80 °C under an atmosphere of Ar, and 29.5 g (0.116 mol) of I_2 was added in one portion under efficient stirring. The cooling bath was removed, and the mixture was allowed to warm to room temperature. The mixture was diluted with 600 mL of ether, the organic layer was washed with aqueous $Na_2S_2O_3$ solution and with H_2O and dried with Na_2SO_4, and the solvents were removed on a rotary evaporator, yielding 31.078 g (0.100 mol, 86%) of iodoferrocene as an orange-brown oil, which solidifies on standing (mp 42−45 °C). Spectroscopic properties concur with published data.[27,30]

***N*-Ferrocenyl Phthalimide (CA #1294-21-9).** A modified and optimized[10,11] procedure was used, avoiding the necessity of ferrocene boronic acid[12] as the precursor of *N*-ferrocenyl phthalimide. A mixture of 80 mL of dry, deoxygenated pyridine, 13.32 g (0.043 mol) of iodoferrocene, 6.91 g (0.070 mol) of phthalimide, and 3.05 g (0.021 mol) of Cu_2O was refluxed for 48 h under an atmosphere of Ar. Solvents and volatile materials were removed on a rotary evaporator, and the residue was triturated with *n*-hexane and filtered through a short Al_2O_3 column. Repeated washings with portions of *n*-hexane removed all the unreacted iodoferrocene, and elution with ether afforded a red solution of the crude product. The solution was dried with Na_2SO_4, and the solvent was removed on a rotary evaporator, yielding the crude product. Recrystallization from ethanol afforded 26.575 g (0.080 mol, 81%) of red crystalline *N*-ferrocenyl phthalimide. Because no spectroscopic properties have been reported in the literature,[10−12] we include these data: red crystals, mp 148−151 °C (lit.[10] mp 156−157 °C). IR (KBr): cm^{-1} 3139 w, 3093 w, 3066 w, 1775 m, 1717 s, 1652 m, 1607 m, 1478 s, 1385 m, 1371 s, 1362 s, 1075 s, 880 s, 808 s, 716 s, 498 s. MS (EI, 70 eV): *m*/*z*(%) 331(100) (M^+), 266(84) (M^+ − Cp), 210(73) (M^+ − FeCp), 185(29) (Fc^+). ^{1}H NMR ($CDCl_3$): δ 4.17 (s, 5H, $Cp_{unsubst}$), 4.19 (m, 2H, Cp_{subst}), 4.98 (m, 2H, Cp_{subst}), 7.72 (m, 2H, phenylene), 7.86 (m, 2H, phenylene). ^{13}C NMR ($CDCl_3$): δ 62.8 (Cp_{subst}), 65.5 (Cp_{subst}), 69.5 ($Cp_{unsubst}$), 123.2 (phenylene), 131.9 (phenylene), 165.1 (C═O), 167.0 (C═O).

Aminoferrocene (CA #1273-82-1). A modified[12] and optimized[10] procedure was used. A mixture of 50 mL of Ar-saturated ethanol, 3.578 g (0.011 mol) of *N*-ferrocenyl phthalimide, and 20 mL of hydrazine hydrate was refluxed under Ar for 2 h. The mixture was cooled to ambient temperature, H_2O was added, and the product was extracted with ether (without protection from air). The yellow organic layer was dried over Na_2SO_4, transferred to a storage Schlenk vessel, and evaporated to dryness, yielding 2.1 g (0.010 mol, 96.8%) of bright yellow aminoferrocene, which was stored and kept in a Schlenk tube under an atmosphere of Ar. Aminoferrocene prepared according to the above procedure showed spectroscopic properties in consonance with published data.[31]

***N*,*N*′-Diferrocenyldiazabutadiene (1)**. A mixture of 0.86 g (4.3 mmol) of aminoferrocene, 40 mL of acetone, 30 mL of H_2O, and 0.3 g (2.1 mmol) of 40% aqueous glyoxal was stirred for 12 h. Addition of 200 mL of H_2O precipitated the purple product, which was filtered off, washed with three portions of H_2O, and dried, yielding 0.86 g (2.0 mmol, 94.8%) of **1**: purple crystals, mp 200 °C (dec). Anal. Found: C, 62.27; H, 4.77. $C_{22}H_{20}Fe_2N_2$ calcd: C, 62.31; H, 4.75. IR (KBr): cm^{-1} 1634 s (C═N), 1497 w, 1233 w, 1105 s, 1038 m, 1025 s, 1003 s, 936 m, 924 m, 820 s, 544 w, 501 s, 488 s, 469 m. MS (EI, 70 eV): *m*/*z*(%) 424(100) M^+, 359(14) (M^+ − Cp), 303(23) (M^+ − FeCp), 201(13) ($FcNH_2^+$), 186(14) (Fc^+), 121(24) ($FeCp^+$). ^{1}H NMR ($CDCl_3$): δ 4.19 (s, 10H, $Cp_{unsubst}$), 4.38 (m, 4H, Cp_{subst}), 4.63 (m, 4H, Cp_{subst}), 8.33 (s, 2H, −N═CH−). ^{13}C NMR (CD_2Cl_2): δ 63.8 (Cp_{subst}), 69.1 (Cp_{subst}), 70.07 ($Cp_{unsubst}$), 102.6 (C(1) of Cp_{subst}), 157.8 (−N═CH−). UV−vis (THF): nm(ϵ) 335(12050), 524(3260).

***N*,*N*′-Diferrocenylethylenediamine (2).** A solution of 0.25 g (0.6 mmol) of **1** in 20 mL of THF was cooled to 0 °C, and 22 mg (0.6 mmol) of $LiAlH_4$ was added. The mixture was stirred at room temperature for 15 min. Aqueous workup yielded 0.21 g (0.5 mmol, 83.2%) of **2**: yellow crystals, mp 150 °C (dec). Anal. Found: C, 61.68; H, 5.66. $C_{22}H_{24}Fe_2N_2$ calcd: C, 61.72; H, 5.65. IR (KBr): cm^{-1} 3341 w (N−H), 3091 w, 2921 w, 1645 w, 1514 s, 1489 s, 1478 m, 1385 w, 1261 s, 1103 s, 1088 s, 1034 s, 1020 s, 1001 m, 800 s, 634 w, 611 w, 490 m. MS (EI, 70 eV): *m*/*z*(%) 428(18) M^+, 214(35) ($FcNCH_2^+$), 186(100) (Fc^+), 121(77) ($FeCp^+$). ^{1}H NMR (DMSO-d_6): δ 3.03 (s, 4H, CH_2CH_2), 3.80 (m, 4H, Cp_{subst}), 3.86 (m, 4H, Cp_{subst}), 3.94 (s, 2H, N−H), 4.11 (s, 10H, $Cp_{unsubst}$). ^{13}C NMR (DMSO-d_6): δ 46.4 (CH_2), 54.6 (Cp_{subst}), 62.3 (Cp_{subst}), 67.6 ($Cp_{unsubst}$), 112.0 (C(1) of Cp_{subst}).

1,3-Diferrocenylimidazolidine (3). A mixture of 290 mg (0.7 mmol) of **2**, 20 mL of acetone, 10 mL of H_2O, and 3 mL (3.5 mmol) of 35% aqueous formaldehyde soultion was stirred at room temperature for 2 h. Further addition of 50 mL of H_2O precipitated the yellow product, yielding 197 mg (0.45 mmol, 66.0%) of **3**: yellow crystals, mp 150 °C (dec). Anal. Found: C, 62.71; H, 5.52. $C_{23}H_{24}Fe_2N_2$ calcd: C, 62.76; H, 5.50. IR (KBr): cm^{-1} 3079 m, 2896 w, 1518 s, 1505 s, 1489 s, 1470 m, 1379 m, 1286 m, 1165 w, 1103 s, 1067 m, 1026 m, 997 m, 982 w, 814 s, 796 s, 634 m, 509 m, 501 s, 484 s, 466 m. MS (EI, 70 eV): *m*/*z*(%) 440(100) M^+, 254(32) (M^+ − Fc), 186(70) (Fc^+), 121(33) ($FeCp^+$). ^{1}H NMR ($CDCl_3$): δ 3.28 (s, 4H, CH_2CH_2), 3.76 (m, 4H, Cp_{subst}), 3.94 (m, 4H, Cp_{subst}), 4.07 (s, 2H, CH_2), 4.21 (s, 10H, $Cp_{unsubst}$). ^{13}C NMR ($CDCl_3$): δ 49.4 (CH_2CH_2), 55.7 (Cp_{subst}), 63.5 (Cp_{subst}), 67.3 ($Cp_{unsubst}$), 71.2 (N−CH_2−N). Single-crystal structure analysis: Figure 1, Table 2, Supporting Information. CV (CH_2Cl_2, V vs SCE): $E_{1/2}^1 = +0.09$, $E_{1/2}^2 = +0.21$ (Table 5, Figure 7).

1,3-Diferrocenylimidazolinium Tetrafluoroborate (4a), Hexafluorophosphate (4b), and Tetraphenylborate (4c). A mixture of 366 mg (0.8 mmol) of **3** and 275 mg (0.8 mmol) of tritylium tetrafluoroborate in 20 mL of dichloromethane was stirred for 2 h. Addition of 10 mL of ether precipitated the product, which was filtered off and washed with small portions of ether and dichloromethane, yielding 271 mg (0.51 mmol, 61.5%) of **4a**. Similarly, a mixture of 540 mg (1.2 mmol) of **3** and 476 mg (1.2 mmol) of tritylium tetrafluoroborate in 40 mL of dichloromethane was stirred for 2 h. Addition of 40 mL of

(29) Fish, R. W.; Rosenblum, M. *J. Org. Chem.* **1965**, *30*, 1253.
(30) Kamounah, F. S.; Christensen, J. B. *J. Chem. Res., Synop.* **1997**, 150.
(31) Herberhold, M.; Ellinger, M.; Kremnitz, W. *J. Organomet. Chem.* **1983**, *241*, 227.

ether precipitated the product, which was filtered off and washed with small portions of ether and dichloromethane, yielding 560 mg (0.96 mmol, 78.1%) of **4b**. Conversion of tetrafluoroborate **4a** to tetraphenylborate **4c**: A solution of 450 mg (1.9 mmol) of **4a** in 700 mL of methanol was combined with a solution of 684 mg (2 mmol) of sodium tetraphenylborate in 5 mL of methanol. The precipitated product was filtered off and washed with three portions of methanol and with two portions of ether, yielding 716 mg (0.95 mmol, 50.0%) of **4c**.

Data for 4a: Yellow crystals, mp 260 °C (dec). IR (KBr): cm^{-1} 3110 w, 1647 s, 1479 m, 1410 w, 1377 w, 1290 s, 1124 m, 1105 s, 1084 s, 1063 s, 1036 s, 1016 m, 999 m, 850 w, 841 w, 814 m, 802 w, 515 w. MS (FAB): *m*/*z*(%) 439(100) (M^+ of cation).

Data for 4b: Yellow crystals, mp 200 °C (dec). IR (KBr): cm^{-1} 3121 w, 1642 s, 1559 w, 1485 w, 1476 m, 1454 w, 1412 w, 1379 w, 1304 w, 1277 s, 1219 w, 1007 m, 1032 w, 1003 w, 856 s, 833 s, 821 s, 557 s, 511 m, 499 m, 490 s, 461 w. MS (FAB): *m*/*z*(%) 439(100) (M^+ of cation). Single-crystal structure analysis: Figure 2, Table 2, Supporting Information.

Data for 4c: Yellow crystals, mp 228 °C (dec). Anal. Found: C, 74.39; H, 5.75. $C_{47}H_{43}BFe_2N_2$ calcd: C, 74.44; H, 5.72. IR (KBr): cm^{-1} 3056 w, 1626 s, 1580 m, 1476 s, 1425 m, 1302 m, 1267 s, 1105 m, 1032 m, 1001 m, 843 m, 827 s, 814 s, 748 s, 733 s, 710 s, 511 s, 492 s, 465 m, 424 w. MS (FAB): *m*/*z*(%) 439(100) (M^+ of cation). ^{1}H NMR (CD_3CN): δ 4.26 (m, 4H, Cp_{subst}), 4.32 (s, 4H, CH_2CH_2), 4.33 (s, 10H, $Cp_{unsubst}$), 4.55 (m, 4H, Cp_{subst}), 6.81−7.27 (m, 20H, tetraphenylborate), 8.31 (s, 1H, N═CH−N). ^{13}C NMR (CD_3CN): δ 50.4 (CH_2CH_2), 60.6 (Cp_{subst}), 67.6 (Cp_{subst}), 70.7 ($Cp_{unsubst}$), 95.1 (C(1) of Cp_{subst}); 122.7, 126.4, 136.6 (tetraphenylborate); 151.3 (N═CH−N). CV (CH_2Cl_2, V vs SCE): $E_{1/2}^1 = +0.53$, $E_{1/2}^2 = +0.65$ (Table 5).

1,3-Diferrocenylimidazoline-2-thione (5). Method A: To a solution of 0.8 g (1.87 mmol) of **2** in 30 mL of toluene was added 0.52 mL (3.73 mmol) of triethylamine and 0.142 mL (1.87 mmol) of thiophosgene, and the mixture was stirred at ambient temperature for 3 days. Aqueous workup and chromatography (Al_2O_3/CH_2Cl_2/ethyl acetate) yielded 415 mg (0.9 mmol, 47.3%) of **5**. Method B: A solution of 60 mg (0.11 mmol) of **4a** in 100 mL of THF was cooled to −80 °C, 0.057 mL (0.11 mmol) of LDA and 0.15 g (0.6 mmol) of sulfur were added, and the mixture was allowed to stir for 2 h. Aqueous workup and chromatography (Al_2O_3/ ether/hexane) yielded 30 mg (0.06 mmol, 56%) of **5**: orange crystals, mp 296 °C. Anal. Found: C, 58.71; H, 4.71. $C_{23}H_{22}Fe_2N_2S$ calcd: C, 58.75; H, 4.72. IR (KBr): cm^{-1} 3100 w, 3085 w, 1489 s, 1431 m, 1418 m, 1408 w, 1389 w, 1377 w, 1308 m, 1296 s, 1202 m, 1105 m, 1095 w, 1030 m, 999 w, 862 w, 833 w, 825 w, 806 m, 499 s, 484 s. MS (EI, 70 eV): *m*/*z*(%) 470(100) (M^+), 405(90) (M^+ − Cp), 121-(33) ($FeCp^+$). ^{1}H NMR ($CDCl_3$): δ 4.01 (s, 4H, CH_2CH_2), 4.09 (m, 4H, Cp_{subst}), 4.21 (s, 10H, $Cp_{unsubst}$), 4.86 (m, 4H, Cp_{subst}). ^{13}C NMR ($CDCl_3$): δ 48.8 (CH_2), 62.5 (Cp_{subst}), 64.9 (Cp_{subst}), 68.9 ($Cp_{unsubst}$). Single-crystal structure analysis: Figure 3, Table 3, Supporting Information. CV (CH_2Cl_2, V vs SCE): $E_{1/2}^1 = +0.31$, $E_{1/2}^2 = +0.43$ (Table 5).

1,3-Diferrocenylimidazolium Trifluoromethansulfonate (6). A Schlenk vessel was charged with 40 mL of acetonitrile and 2.4 mL (2.4 mmol) of $ZnEt_2$ (1.0 M solution in hexane). After cooling to −80 °C, 0.42 mL (4.74 mmol) of triflic acid was added dropwise, and the flask was allowed to warm to room temperature under efficient stirring. Addition of 1.0 g (2.36 mmol) of **1** caused an immediate color change from dark purple to green. Stirring was continued for 15 min, and 70 mg (2.34 mmol) of paraformaldehyde was added. The mixture was stirred for 3 days and worked up. All volatile materials were removed on a rotary evaporator, and the residue was dissolved in dichloromethane and chromatographed (Al_2O_3, CH_2Cl_2/CH_3CN; 4:1), yielding 372 mg (0.63 mmol, 26.9%) of **6**: yellow crystals, mp 229 °C (dec). Anal. Found: C, 49.21; H, 3.63. $C_{24}H_{21}F_3Fe_2O_3N_2S$ calcd: C, 49.17; H, 3.61. IR (KBr): cm^{-1} 3062 m, 2927 w, 1566 m, 1283 s, 1265 s, 1231 w, 1165 m, 1150 m, 1105 w, 1095 w, 1086 w, 1034 s, 1003 w, 872 w, 843 w, 816 m, 756 w, 650 s, 634 w, 519 m, 505 m, 486 w. MS (FAB): *m*/*z*(%) 437(100) (M^+ of cation). ^{1}H NMR (CD_3CN): δ 4.32 (s, 10H, $Cp_{unsubst}$), 4.40 (m, 4H, Cp_{subst}), 4.91 (m, 4H, Cp_{subst}), 7.80 (s, 2H, −CH═CH−), 9.05 (s, 1H, −N−CH═N−). ^{13}C NMR (CD_3CN): δ 63.3 (Cp_{subst}), 68.4 (Cp_{subst}), 71.4 ($Cp_{unsubst}$), 92.1 (C(1) of Cp_{subst}), 123.8 (−CH═CH−), 134.4 (N−CH═N−).

1,3-Diferrocenylimidazolium Tetraphenylborate (7). A solution of 15 mg (0.025 mmol) of **6** in 2 mL of methanol was combined with a solution of 30 mg (0.067 mmol) of sodium tetraphenylborate in 1 mL of methanol. The precipitated product was filtered off and washed with three portions of methanol, yielding 10 mg (0.013 mmol, 52%) of **7**: yellow crystals, mp 230 °C (dec). Anal. Found: C, 74.60; H, 5.47. $C_{47}H_{41}BFe_2N_2$ calcd: C, 74.64; H, 5.46. IR (KBr): cm^{-1} 3056 w, 3002 w, 1557 s, 1478 m, 1263 m, 1105 s, 1092 s, 1078 s, 1030 s, 1001 s, 868 s, 858 s, 841 s, 829 s, 748 s, 733 s, 712 s, 700 s, 640 s, 613 s, 511 s, 493 s, 465 s. MS (FAB): *m*/*z*(%) 437(100) (M^+ of cation). ^{1}H NMR (CD_3CN): δ 4.32 (s, 10H, $Cp_{unsubst}$), 4.40 (m, 4H, Cp_{subst}), 4.86 (m, 4H, Cp_{subst}), 6.70−7.26 (m, 20H, phenyl), 7.76 (s, 2H, −CH═CH−), 8.93 (s, 1H, −N−CH═N−). ^{13}C NMR (CD_3CN): δ 63.2 (Cp_{subst}), 68.3 (Cp_{subst}), 71.2 ($Cp_{unsubst}$), 93.1 (C(1) of Cp_{subst}), 122.6 (phenyl), 123.9 (−CH═CH−), 126.4 (phenyl), 126.5 (phenyl), 126.6 (phenyl), 134.5 (N−CH═N−), 136.7 (phenyl), 156.6 (phenyl). Single-crystal structure analysis: Figure 4, Table 3, Supporting Information. CV (CH_2Cl_2, V vs SCE): $E_{1/2}^1 = +0.75$, $E_{1/2}^2 = +0.75$ (Table 5).

1,3-Diferrocenylimidazole-2-thione (8). A solution of 117 mg (0.15 mmol) of **7** in 20 mL of THF was cooled to −80 °C, and 0.1 mL (0.15 mmol) of a 1.5 M hexane solution of methyllithium and, after the mixture had warmed to room temperature, 5 mg (0.020 mmol) of sulfur were added. The mixture was allowed to stir for 2 h. Aqueous workup yielded 32 mg (0.068 mmol, 44.2%) of **8**: orange crystals, mp 251 °C. Anal. Found: C, 58.88; H, 4.30. $C_{23}H_{20}Fe_2N_2S$ calcd: C, 59.00; H, 4.31%. IR (KBr): cm^{-1} 2967 w, 1674 w, 1647 m, 1497 s, 1408 m, 1369 m, 1346 m, 1327 s, 1269 w, 1207 w, 1150 w, 1119 m, 1026 w, 999 m, 868 s, 841 m, 806 s, 713 m, 659 w, 486 s. MS (EI, 70 eV): *m*/*z*(%) 468(100) (M^+), 403(100) (M^+ − Cp), 347(11) (M^+ − FeCp), 338(38) (M^+ − 2 Cp), 282(18) (M^+ − FeCp, Cp). ^{1}H NMR (CD_2Cl_2): δ 4.24 (m, 4H, Cp_{subst}), 4.28 (s, 10H, $Cp_{unsubst}$), 4.87 (m, 4H, Cp_{subst}), 7.14 (s, 2H, −CH═CH−). ^{13}C NMR ($CDCl_3$): δ 65.9 (Cp_{subst}), 68.2 (Cp_{subst}), 69.9 ($Cp_{unsubst}$), 95.4 (C(1) of Cp_{subst}), 119.2 (CH═CH). Single-crystal structure analysis: Figure 5, Table 4, Supporting Information. CV (CH_2Cl_2, V vs SCE): $E_{1/2}^1 = +0.46$, $E_{1/2}^2 = +0.55$ (Table 5).

Bis[1,3-diferrocenylimidazol-2-ylidene]silver(I) Tetraphenylborate (9). A mixture of 123 mg (0.16 mmol) of **7** in 30 mL of dichloromethane, 19 mg (0.08 mmol) of Ag_2O, 100 mg (2.5 mmol) of NaOH in 3 mL of H_2O, and 15 mg (0.027 mmol) of tetrabutylammonium tetraphenylborate was stirred for 48 h. The organic layer was separated from the aqueous layer and filtered to remove solid byproducts. Addition of hexane precipitated the crude product, which was repeatedly dissolved in dichloromethane and precipitated with hexane to afford 133 mg (0.1 mmol, 62.9%) of **9**: yellow crystals, mp > 200 °C (dec). Anal. Found: C, 64.45; H, 4.67. $C_{70}H_{60}AgBFe_4N_4$ calcd: C, 64.71; H, 4.65%. IR (KBr): cm^{-1} 3093 w, 2983 w, 1582 m, 1497 s, 1479 s, 1458 m, 1427 w, 1381 w, 1107 m, 1032 m, 1001 w, 872 m, 843 m, 821 m, 767 s, 733 s, 609 m, 511 w, 490 m, 470 w. Raman (single crystal, 785 nm): cm^{-1} 1100, 992, 427, 366, 351, 324, 296, 265, 190, 157, 70. HRMS (ESI): *m*/*z* = 978.9713 (calc: 978.9700) (M^+ of cation). ^{1}H NMR (CD_2Cl_2): δ 4.25 (m, 8H, Cp_{subst}), 4.30 (s, 20H, $Cp_{unsubst}$), 4.63 (m, 8H, Cp_{subst}), 6.9−7.4 (m, 20H, phenyl); 7.43 (d, 4H, $^4J(^1H-^{107/109}Ag) = 1.4$ Hz, −CH═CH−). ^{13}C NMR (CD_2Cl_2): δ 64.3 (Cp_{subst}), 67.2 (Cp_{subst}), 70.4 ($Cp_{unsubst}$), 97.9 (d, $^3J(^{13}C-^{107/109}Ag = 1.0$ Hz, C(1) of Cp_{subst}); 122.1 (C(4) of phenyl);

123.4 (d, $^{3}J(^{13}C-^{107/109}Ag = 5.7$ Hz, C(4,5) of imidazole); 126.0 (q, $^{2}J(^{11}B-^{13}C = 2.6$ Hz, C(2,6) of phenyl); 136.3 (q, $^{3}J(^{11}B-^{13}C = 1.4$ Hz, C(3,5) of phenyl); 164.4 (q × sep, $^{1}J(^{11}B-^{13}C) = 49.3$ Hz, $^{1}J(^{10}B-^{13}C) = 16.5$ Hz, C(1) of phenyl); 180.6 (d × d, $^{1}J(^{13}C-^{107}Ag) = 188.9$ Hz, $^{1}J(^{13}C-^{109}Ag) = 218.6$ Hz, C(2) of imidazole). INEPT ^{109}Ag NMR (CD_2Cl_2): δ 727 (unresolved quintet with $^{4}J(^{1}H-^{107/109}Ag = 1.6$ Hz). Single-crystal structure analysis: Figure 6, Table 4, Supporting Information. CV (CH_2Cl_2, V vs SCE): $E_{1/2} = +0.8$ (Figure 8, Supporting Information).

Acknowledgment. We thank the FWF (P12319-PHY and P13073-PHY), Vienna, Austria, for funding of the Raman spectrometer. P.Z. gratefully acknowledges the financial support of the University of Siena (ex quota 60%), and G.O. acknowledges a one-year scholarship from CIRCSMB.

Supporting Information Available: Figure 8 and tables of crystal data and structure refinement details, anisotropic thermal parameters, fractional atomic parameters, isotropic thermal parameters for the non-hydrogen atoms, all bond lengths and angles, and fractional atomic coordinates for the hydrogen atoms for **3**, **4b**, **5**, **7**, **8**, and **9**. This material is available free of charge via the Internet at http://pubs.acs.org.

OM990377H